EUROPEAN JOURNAL OF PURE AND APPLIED MATHEMATICS
2025, Vol. 18, Issue 4, Article Number 7172
ISSN 1307-5543 – ejpam.com
Published by New York Business Global

New Trigonometric and Hyperbolic Stochastic Fractional Solutions for the Conformable Derivative Coupled Schrödinger-KdV Equations Using Sardar Subequation Method

Wael W. Mohammed[1,*], Naveed Iqbal[1], Hijyah M. Alshammary[1], F. Gassem[1], Mohamed S. Algolam[1]

[1] *Department of Mathematics, College of Science, University of Ha'il, Ha'il 2440, Saudi Arabia*

Abstract. In this paper, we look at the stochastic coupled Schrödinger-KdV equations with conformable derivative operator (SCS-KdVEs-CDO). By using the Sardar subequation method (SS-method), we can obtain results such as periodic soliton, bright soliton, dark-bright soliton and singular soliton. Some previous solutions of coupled Schrödinger-KdV equations are obtained when the order of derivatives is integer and noise is ignored. Due to the important applications of the coupled Schrödinger-KdV equations in dusty plasma, such as dust-acoustic waves, electromagnetic waves, and Langmuir waves, these obtained solutions might be utilized to the analysis of many fundamental physical phenomena. Furthermore, the effects of the conformable derivative operator and the noise term on the analytical solution of the SCS-KdVEs-CDO were illustrated by simulating some solutions via the MATLAB program.

2020 Mathematics Subject Classifications: 35A20, 60H10, 60H15, 35Q51, 35Q80

Key Words and Phrases: Exact solutions, stochastic process, stochastic soliton solutions, stability by noise

1. Introduction

Fractional partial differential equations (FPDEs) represent a powerful mathematical tool for modeling and understanding complex systems. By incorporating fractional derivatives, these equations can capture the non-local and memory effects that are often present in real-world phenomena. As research in this area continues to advance, we can anticipate seeing even more applications of fractional partial differential equations in various engineering and scientific disciplines. Recently, numerous powerful approaches for discovering

*Corresponding author.
DOI: https://doi.org/10.29020/nybg.ejpam.v18i4.7172

Email addresses: w.mohammed@uoh.edu.sa (W. W. Mohammed), n.iqbal@uoh.edu.sa (N. Iqbal)

exact solutions to PDEs have been introduced, such as sine-Gordon expansion technique [1], modified mapping method [2], F-expansion method [3, 4], (G'/G)-expansion [5, 6], sine-cosine method [7], modified extended tanh-function method [8], exp-function method [9], $exp(-\phi(\varsigma))$-expansion method [10], Riccati equation method [11], Jacobi elliptic function expansion [12], the Riccati-Bernoulli sub-ODE method [13, 14] and etc.

One of these equations is coupled Schrödinger-KdV (CS-KDV) equation . The CS-KDV equations are a powerful mathematical model that combines the KdV equation and the Schrödinger equation to describe the interaction between nonlinear waves and quantum particles. This equation offers a flexible and accurate framework for studying a wide range of physical phenomena, including solitons, quantum chaos, and complex wave dynamics. By incorporating conformable derivative operator, the CS-KDV equations provides a versatile tool for researchers in various scientific disciplines to explore the intricate relationships between quantum mechanics and nonlinear wave propagation.

On other side, including a random term into coupled Schrödinger-KdV equations is important because it introduces an element of realism and flexibility. In real-world scenarios, systems often experience random disturbances and fluctuations, such as noise or variability in the environment. By incorporating a random term, mathematicians and physicists can simulate and analyze how these unpredictable influences affect the behavior and evolution of waves within these systems. This enhances the accuracy and reliability of the models used to predict wave phenomena..

Here, we take into account the stochastic coupled Schrödinger-KdV equations with conformable derivative operator (SCS-KdVEs-CDO) as follows:

$$\begin{aligned} &\mathcal{Z}_t + 6\mathcal{Z}\mathcal{T}_x^{\alpha}\mathcal{Z} + \mathcal{T}_{xxx}^{\alpha}\mathcal{Z} = \mathcal{T}_x^{\alpha}\left(|\mathcal{Y}|^2\right) + \rho\mathcal{Z}\mathcal{W}_t, \\ &i\mathcal{Y}_t = \mathcal{T}_{xx}^{\alpha}\mathcal{Y} - \mathcal{Y}\mathcal{Z} + i\rho\mathcal{Y}\mathcal{W}_t, \end{aligned} \tag{1}$$

where $\mathcal{Z}(x,t)$ is the real-valued function and presents a long wave profile while $\mathcal{Y}(x,t)$ is the complex function and presents the short wave profile; $\mathcal{T}^{\alpha}$ is the conformable derivative operator [15] for $0 < \alpha \leq 1$; ρ is the amplitude of noise; $\mathcal{W}$ is a standard Wiener process and $\mathcal{W}_t = \frac{\partial \mathcal{W}}{\partial t}$.

Due to the importance of the CS-KdV equation in soliton theory, mathematical physics and hydrodynamics, many authors have obtained its solutions by applying different methods, including mapping method [16], finite element method [17] Kudryashov method [18], adomian's decomposition method [19], Petrov-Galerkin Method [20], F-expansion method [21], complex hyperbolic-function method [22], (G'/G)-expansion method [23], $\exp(-\varphi(\xi))$-expansion method [24], and the mapping method [25]. While the stochastic coupled Schrödinger-KdV equations with conformable derivative operator have not been investigated before.

Our novelty of this work is to obtain the exact solutions for the SCS-KdVEs-CDO (1). The Sardar subequation method (SS-Method) is used to find various types of solutions such as periodic soliton, bright soliton, dark-bright soliton and singular soliton. Moreover, we provide a number of three-and two-dimensional graphs to examine how the Wiener

process term affects on the obtained solutions. Also, we generalize some early results such as the results stated in [16, 21].

The following is an outline of the paper: The SCS-KdVEs-CDO (1) wave equation is given in Sec. 2 , while Sec. 3 states the Sardar subequation method. In Sec. 4, we get the solutions of (1). In Sec. 5, we address the effect of the Wiener process term on the solutions of the SCS-KdVEs-CDO (1). The results acquired for this research are finally given.

2. Traveling Wave Equation for the SCS-KdVEs-CDO

To have the wave equation for the SCS-KdVEs-CDO (1), we apply

$$\mathcal{Y}(x,t)=u(\zeta)e^{i\Theta+\rho\mathcal{W}-\frac{1}{2}\rho^2t} \text{ and } \mathcal{Z}(x,t)=v(\zeta)e^{\rho\mathcal{W}-\frac{1}{2}\rho^2t}, \tag{2}$$

$$\Theta=\frac{k}{\alpha}x^{\alpha}+\delta t,\ \zeta=\frac{1}{\alpha}x^{\alpha}+2kt,$$

where u and v are deterministic and real functions; k and δ are non-zero real constants. It is observed that

$$\begin{aligned}\mathcal{Y}_t &= [2ku'+i\delta u+\rho u\mathcal{W}_t-\frac{1}{2}\rho^2u+\frac{1}{2}\rho^2u]e^{i\Theta+\rho\mathcal{W}-\frac{1}{2}\rho^2t}\\ &= [2ku'+i\delta u+\rho u\mathcal{W}_t]e^{i\Theta+\rho\mathcal{W}-\frac{1}{2}\rho^2t},\\ \mathcal{Y}_x &= (u'+iku)e^{i\Theta+\rho\mathcal{W}-\frac{1}{2}\rho^2t},\ \mathcal{Y}_{xx}=(u''+2iku'-k^2u)e^{i\Theta+\rho\mathcal{W}-\frac{1}{2}\rho^2t},\end{aligned} \tag{3}$$

where $\frac{1}{2}\rho^2u$ is the Itô correction term. Similarly,

$$\mathcal{Z}_t=[2kv'+\rho v\mathcal{W}_t]e^{\rho\mathcal{W}-\frac{1}{2}\rho^2t},\ \mathcal{Z}_x=v'e^{\rho\mathcal{W}-\frac{1}{2}\rho^2t},\ \mathcal{Z}_{xxx}=v'''e^{\rho\mathcal{W}-\frac{1}{2}\rho^2t}. \tag{4}$$

Substituting Eqs (2), (3) and (4) into Eq. (1), we have the next system:

$$\begin{aligned}&2kv`+v```+[6vv`-\left(u^2\right)`]e^{\rho\mathcal{W}-\frac{1}{2}\rho^2t}=0,\\ &u``+\left(\delta-k^2\right)u+uve^{\rho\mathcal{W}-\frac{1}{2}\rho^2t}=0.\end{aligned} \tag{5}$$

Considering the expectation on both sides of Eq. (5), yields

$$\begin{aligned}&2kv`+v```+[6vv`-\left(u^2\right)`]e^{-\frac{1}{2}\rho^2t}\mathbb{E}(e^{\rho\mathcal{W}})=0,\\ &u``+\left(\delta-k^2\right)u+uve^{-\frac{1}{2}\rho^2t}\mathbb{E}(e^{\rho\mathcal{W}})=0.\end{aligned} \tag{6}$$

Since $\mathcal{W}(t)$ is a Wiener process, hence $\mathbb{E}(e^{\rho\mathcal{W}(t)})=e^{\frac{1}{2}\rho^2t}$ for any real number ρ. Therefore, Eq. (6) tends into

$$\begin{aligned}&2kv`+v```+6vv`-\left(u^2\right)`=0,\\ &u``+\left(\delta-k^2\right)u+uv=0.\end{aligned} \tag{7}$$

Integrating first equation in Eq. (7) once, we get

$$\begin{aligned} v'' + 2kv + 3v^2 - u^2 = 0, \\ u''' + \left(\delta - k^2\right) u + uv = 0. \end{aligned} \tag{8}$$

3. The clarification of SS-method

Let us describe the SS-method that we use here (for more detail see [16, 26]). Let the solution of Eq. (8) have the form

$$\begin{aligned} u(\zeta) = \sum_{i=0}^{m_1} \ell_i \mathcal{F}^i(\zeta), \\ v(\zeta) = \sum_{i=0}^{m_2} \varpi_i \mathcal{F}^i(\zeta), \end{aligned} \tag{9}$$

where ℓ_i and ϖ_i are undetermined constants to be established, and $\mathcal{F}$ solves the auxiliary equation:

$$(\mathcal{F}')^2 = \mathcal{F}^4 + \hbar_1 \mathcal{F}^2 + \hbar_2, \tag{10}$$

where $\hbar_1$, and $\hbar_2$ are real constants. Many cases rely on $\hbar_1$, and $\hbar_2$ for the solutions of Eq. (10) as follows:

Case 1: If $\hbar_1 > 0$, and $\hbar_2 = 0$, then

$$\mathcal{F}_1(\zeta) = \pm\sqrt{pq\hbar_1}\,\mathrm{sech}_{pq}(\sqrt{\hbar_1}\zeta), \tag{11}$$

and

$$\mathcal{F}_2(\zeta) = \pm\sqrt{pq\hbar_1}\,\mathrm{csch}_{pq}(\sqrt{\hbar_1}\zeta), \tag{12}$$

where

$$\mathrm{sech}_{pq}(\theta) = \frac{2}{pe^{\theta} + qe^{-\theta}} \quad \text{and} \quad \mathrm{csch}_{pq}(\theta) = \frac{2}{pe^{\theta} - qe^{-\theta}}.$$

Case 2: If $\hbar_1 < 0$, and $\hbar_2 = 0$, then

$$\mathcal{F}_3(\zeta) = \pm\sqrt{-pq\hbar_1}\,\mathrm{sec}_{pq}(\sqrt{-\hbar_1}\zeta), \tag{13}$$

and

$$\mathcal{F}_4(\zeta) = \pm\sqrt{-pq\hbar_1}\,\mathrm{csc}_{pq}(\sqrt{-\hbar_1}\zeta), \tag{14}$$

where

$$\mathrm{sec}_{pq}(\theta) = \frac{2}{pe^{\theta i} + qe^{-\theta i}} \quad \text{and} \quad \mathrm{csc}_{pq}(\theta) = \frac{2}{pe^{\theta i} - qe^{-\theta i}}.$$

Case 3: If $\hbar_1 < 0$, and $\hbar_2 = \frac{\hbar_1^2}{4}$, then

$$\mathcal{F}_5(\zeta) = \pm\sqrt{\frac{-\hbar_1}{2}}\,\tanh_{pq}(\sqrt{\frac{-\hbar_1}{2}}\zeta), \tag{15}$$

$$\mathcal{F}_6(\zeta) = \pm\sqrt{\frac{-\hbar_1}{2}}\coth_{pq}(\sqrt{\frac{-\hbar_1}{2}}\zeta), \tag{16}$$

$$\mathcal{F}_7(\zeta) = \pm\sqrt{\frac{-\hbar_1}{2}}[\coth_{pq}(\sqrt{-2\hbar_1}\zeta) \pm \sqrt{pq}\operatorname{csch}_{pq}(\sqrt{-2\hbar_1}\zeta)], \tag{17}$$

and

$$\mathcal{F}_8(\zeta) = \pm\sqrt{\frac{-\hbar_1}{8}}[\tanh_{pq}(\sqrt{\frac{-\hbar_1}{8}}\zeta) + \coth_{pq}(\sqrt{\frac{-\hbar_1}{8}}\zeta)], \tag{18}$$

where

$$\tanh_{pq}(\theta) = \frac{pe^{\theta} - qe^{-\theta}}{pe^{\theta} + qe^{-\theta}} \text{ and } \coth_{pq}(\theta) = \frac{pe^{\theta} + qe^{-\theta}}{pe^{\theta} - qe^{-\theta}}.$$

Case 4: If $\hbar_1 > 0$, and $\hbar_2 = \frac{\hbar_1^2}{4}$, then

$$\mathcal{F}_9(\zeta) = \pm\sqrt{\frac{\hbar_1}{2}}\tan_{pq}(\sqrt{\frac{\hbar_1}{2}}\zeta), \tag{19}$$

$$\mathcal{F}_{10}(\zeta) = \pm\sqrt{\frac{\hbar_1}{2}}\cot_{pq}(\sqrt{\frac{\hbar_1}{2}}\zeta), \tag{20}$$

$$\mathcal{F}_{11}(\zeta) = \pm\sqrt{\frac{\hbar_1}{2}}[\tan_{pq}(\sqrt{2\hbar_1}\zeta) \pm \sqrt{pq}\sec_{pq}(\sqrt{2\hbar_1}\zeta)], \tag{21}$$

$$\mathcal{F}_{12}(\zeta) = \pm\sqrt{\frac{\hbar_1}{2}}[\cot_{pq}(\sqrt{2\hbar_1}\zeta) \pm \sqrt{pq}\csc_{pq}(\sqrt{2\hbar_1}\zeta)], \tag{22}$$

and

$$\mathcal{F}_{13}(\zeta) = \pm\sqrt{\frac{\hbar_1}{8}}[\tan_{pq}(\sqrt{\frac{\hbar_1}{8}}\zeta) + \cot_{pq}(\sqrt{\frac{\hbar_1}{8}}\zeta)], \tag{23}$$

where

$$\tan_{pq}(\theta) = -i\frac{pe^{\theta i} - qe^{-\theta i}}{pe^{\theta i} + qe^{-\theta i}} \text{ and } \cot_{pq}(\theta) = i\frac{pe^{\theta i} + qe^{-\theta i}}{pe^{\theta i} - qe^{-\theta i}}.$$

4. Exact solutions of the the SCS-KdVEs-CDO

First, let us equate u'' with uv and v'' with v^2 in Eq. (8) to determine the parameters m_1 and m_2 as

$$m_1 = 2 \text{ and } m_2 = 2.$$

With $m_1 = 2$ and $m_2 = 2$, Eq. (9) has the form

$$\begin{aligned} u(\zeta) &= \ell_0 + \ell_1\mathcal{F}(\zeta) + \ell_2\mathcal{F}^2(\zeta), \\ v(\zeta) &= \varpi_0 + \varpi_1\mathcal{F}(\zeta) + \varpi_2\mathcal{F}^2(\zeta). \end{aligned} \tag{24}$$

Substituting Eq. (24) into Eq. (8), we obtain

$$[\ell_2\varpi_2 + 6\ell_2]\mathcal{F}^4 + [2\ell_1 + \ell_1\varpi_2 + \ell_2\varpi_1]\mathcal{F}^3$$

$$
\begin{aligned}
&+[4\hbar_1\ell_2+\left(\delta-k^2\right)\ell_2+\ell_0\varpi_2+\ell_2\varpi_0+\ell_1\varpi_1]\mathcal{F}^2\\
&+[\hbar_1\ell_1+\left(\delta-k^2\right)\ell_1+\ell_1\varpi_0+\ell_0\varpi_1]\mathcal{F}\\
&+[2\hbar_2\ell_2+\left(\delta-k^2\right)\ell_0+\ell_0\varpi_0]=0,
\end{aligned}
$$

and

$$
\begin{aligned}
&(6\varpi_2-\ell_2^2+3\varpi_2^2)\mathcal{F}^4+(2\varpi_1+6\varpi_1\varpi_2-2\ell_1\ell_2)\mathcal{F}^3\\
&+(4\varpi_2\hbar_1+2k\varpi_2+6\varpi_0\varpi_2-2\ell_0\ell_2+3\varpi_1^2-\ell_1^2)\mathcal{F}^2\\
&+(\hbar_1\varpi_1+2k\varpi_1+6\varpi_0\varpi_1-2\ell_0\ell_1)\mathcal{F}\\
&+(2\hbar_2\varpi_2+2k\varpi_0+3\varpi_0^2-\ell_0^2)=0.
\end{aligned}
$$

For $j=4,3,2,1,0$, we balance each coefficient of $\mathcal{F}^j$ with zero to get

$$\ell_2\varpi_2+6\ell_2=0,$$

$$2\ell_1+\ell_1\varpi_2+\ell_2\varpi_1=0,$$

$$4\hbar_1\ell_2+\left(\delta-k^2\right)\ell_2+\ell_0\varpi_2+\ell_2\varpi_0+\ell_1\varpi_1=0,$$

$$\hbar_1\ell_1+\left(\delta-k^2\right)\ell_1+\ell_1\varpi_0+\ell_0\varpi_1=0,$$

$$2\hbar_2\ell_2+\left(\delta-k^2\right)\ell_0+\ell_0\varpi_0=0,$$

and

$$6\varpi_2-\ell_2^2+3\varpi_2^2=0,$$

$$2\varpi_1+6\varpi_1\varpi_2-2\ell_1\ell_2=0,$$

$$4\varpi_2\hbar_1+2k\varpi_2+6\varpi_0\varpi_2-2\ell_0\ell_2+3\varpi_1^2-\ell_1^2=0,$$

$$\hbar_1\varpi_1+2k\varpi_1+6\varpi_0\varpi_1-2\ell_0\ell_1=0,$$

$$2\hbar_2\varpi_2+2k\varpi_0+3\varpi_0^2-\ell_0^2=0.$$

By solving the above equations, we have two sets of solutions as follows:

Set I:

$$
\begin{aligned}
&\ell_0=\ell_2=0,\ \ell_1=\pm2\sqrt{(\hbar_1-k-3k^2+3\delta)},\\
&\varpi_0=k^2-\delta-\hbar_1,\ \varpi_1=0,\ \varpi_2=-2.
\end{aligned}
\tag{25}
$$

Set II:

$$
\begin{aligned}
&\ell_0=\pm2\sqrt{2}\left(10\hbar_1-\sqrt{\hbar_1-3\hbar_2}\right),\ \ell_1=0,\ \ell_2=\pm6\sqrt{2}\\
&\varpi_0=-(2\hbar_1+\tfrac{1}{3}k+\tfrac{4}{3}\sqrt{\hbar_1-3\hbar_2}),\ \varpi_1=0,\ \varpi_2=-6,\\
&\delta=-k^2-\tfrac{1}{3}k\pm\tfrac{10}{3}\sqrt{\hbar_1-3\hbar_2}.
\end{aligned}
\tag{26}
$$

Set I: Plugging (25) into Eq. (24), we obtain the next solution for the traveling wave Eq. (8):

$$u\ =\ \pm2\sqrt{(\hbar_1-k-3k^2+3\delta)}\mathcal{F}\left(\zeta\right),\tag{27}$$

$$v = k^2 - \delta - \hbar_1 - 2\mathcal{F}^2(\zeta),$$

For $\left(\hbar_1 - k - 3k^2 + 3\delta\right) > 0$. Similarly, putting Eq. (27) into equation Eq. (2), we attain the solutions of the SCS-KdVEs-CDO (1) as follows:

$$\begin{aligned} \mathcal{Y}(x,t) &= \pm 2\sqrt{(\hbar_1 - k - 3k^2 + 3\delta)}\mathcal{F}(\zeta)\, e^{i\Theta + \rho\mathcal{W} - \frac{1}{2}\rho^2 t}, \\ \mathcal{Z}(x,t) &= \{k^2 - \delta - \hbar_1 - 2\mathcal{F}^2(\zeta)\} e^{\rho\mathcal{W} - \frac{1}{2}\rho^2 t}, \end{aligned} \tag{28}$$

where $\zeta = \frac{1}{\alpha}x^\alpha + 2kt$ and $\Theta = \frac{k}{\alpha}x^\alpha + \delta t$.

Now, substituting from Eqs (11) to (23) into Eq. (28), we have the next solutions of the the SCS-KdVEs-CDO (1):

Case I-1: If $\hbar_1 > 0$, and $\hbar_2 = 0$, then

$$\mathcal{Y}_{1,1} = \pm 2\sqrt{pq\hbar_1\left(\hbar_1 - k - 3k^2 + 3\delta\right)}\mathrm{sech}_{pq}(\sqrt{\hbar_1}\zeta) e^{i\Theta + \rho\mathcal{W} - \frac{1}{2}\rho^2 t}, \tag{29}$$

$$\mathcal{Z}_{1,1} = \{k^2 - \delta - \hbar_1 - 2pq\hbar_1 \mathrm{sech}^2_{pq}(\sqrt{\hbar_1}\zeta)\} e^{\rho\mathcal{W} - \frac{1}{2}\rho^2 t}, \tag{30}$$

and

$$\mathcal{Y}_{1,2} = \pm 2\sqrt{pq\hbar_1\left(\hbar_1 - k - 3k^2 + 3\delta\right)}\mathrm{csch}_{pq}(\sqrt{\hbar_1}\zeta) e^{i\Theta + \rho\mathcal{W} - \frac{1}{2}\rho^2 t}, \tag{31}$$

$$\mathcal{Z}_{1,2} = \{k^2 - \delta - \hbar_1 - 2pq\hbar_1 \mathrm{csch}^2_{pq}(\sqrt{\hbar_1}\zeta)\} e^{\rho\mathcal{W} - \frac{1}{2}\rho^2 t}, \tag{32}$$

for $\left(\hbar_1 - k - 3k^2 + 3\delta\right) > 0$.

Case I-2: If $\hbar_1 < 0$, and $\hbar_2 = 0$, then

$$\mathcal{Y}_{1,3} = \pm 2\sqrt{-pq\hbar_1\left(\hbar_1 - k - 3k^2 + 3\delta\right)}\,\mathrm{sec}_{pq}(-\sqrt{\hbar_1}\zeta) e^{i\Theta + \rho\mathcal{W} - \frac{1}{2}\rho^2 t}, \tag{33}$$

$$\mathcal{Z}_{1,3} = \{k^2 - \delta - \hbar_1 + 2pq\hbar_1\,\mathrm{sec}^2_{pq}(\sqrt{\hbar_1}\zeta)\} e^{\rho\mathcal{W} - \frac{1}{2}\rho^2 t}, \tag{34}$$

and

$$\mathcal{Y}_{1,4} = \pm 2\sqrt{-pq\hbar_1\left(\hbar_1 - k - 3k^2 + 3\delta\right)}\,\mathrm{csc}_{pq}(-\sqrt{\hbar_1}\zeta) e^{i\Theta + \rho\mathcal{W} - \frac{1}{2}\rho^2 t}, \tag{35}$$

$$\mathcal{Z}_{1,4} = \{k^2 - \delta - \hbar_1 + 2pq\hbar_1\,\mathrm{csc}^2_{pq}(\sqrt{\hbar_1}\zeta)\} e^{\rho\mathcal{W} - \frac{1}{2}\rho^2 t}, \tag{36}$$

for $\left(\hbar_1 - k - 3k^2 + 3\delta\right) > 0$.

Case I-3: If $\hbar_1 < 0$, and $\hbar_2 = \frac{\hbar_1^2}{4}$, then

$$\mathcal{Y}_{1,5} = \pm\sqrt{-2\hbar_1\left(\hbar_1 - k - 3k^2 + 3\delta\right)}\,\tanh_{pq}(\sqrt{\frac{-\hbar_1}{2}}\zeta) e^{i\Theta + \rho\mathcal{W} - \frac{1}{2}\rho^2 t}, \tag{37}$$

$$\mathcal{Z}_{1,5} = \{k^2 - \delta - \hbar_1 + \hbar_1\tanh^2_{pq}(\sqrt{\frac{-\hbar_1}{2}}\zeta)\} e^{\rho\mathcal{W} - \frac{1}{2}\rho^2 t}, \tag{38}$$

$$\mathcal{Y}_{1,6} = \pm\sqrt{-2\hbar_1\left(\hbar_1 - k - 3k^2 + 3\delta\right)}\,\coth_{pq}(\sqrt{\frac{-\hbar_1}{2}}\zeta) e^{i\Theta + \rho\mathcal{W} - \frac{1}{2}\rho^2 t}, \tag{39}$$

$$\mathcal{Z}_{1,6} = \{k^2 - \delta - \hbar_1 + \hbar_1\coth^2_{pq}(\sqrt{\frac{-\hbar_1}{2}}\zeta)\} e^{\rho\mathcal{W} - \frac{1}{2}\rho^2 t}, \tag{40}$$

$$\mathcal{Y}_{1,7}=\pm\sqrt{-2\hbar_1\left(\hbar_1-k-3k^2+3\delta\right)}[\coth_{pq}(\sqrt{-2\hbar_1}\zeta)\pm\sqrt{pq}\mathrm{csch}_{pq}(\sqrt{-2\hbar_1}\zeta)]e^{i\Theta+\rho\mathcal{W}-\frac{1}{2}\rho^2t}, \tag{41}$$

$$\mathcal{Z}_{1,7}=\{k^2-\delta-\hbar_1+\hbar_1[\coth_{pq}(\sqrt{-2\hbar_1}\zeta)\pm\sqrt{pq}\mathrm{csch}_{pq}(\sqrt{-2\hbar_1}\zeta)]^2\}e^{\rho\mathcal{W}-\frac{1}{2}\rho^2t}, \tag{42}$$

and

$$\mathcal{Y}_{1,8}=\pm\frac{1}{2}\sqrt{-\hbar_1\left(\hbar_1-k-3k^2+3\delta\right)}[\tanh_{pq}(\sqrt{\frac{-\hbar_1}{8}}\zeta)+\coth_{pq}(\sqrt{\frac{-\hbar_1}{8}}\zeta)]e^{i\Theta+\rho\mathcal{W}-\frac{1}{2}\rho^2t}, \tag{43}$$

$$\mathcal{Z}_{1,8}=\{k^2-\delta-\hbar_1+\frac{1}{4}\hbar_1[\tanh_{pq}(\sqrt{\frac{-\hbar_1}{8}}\zeta)+\coth_{pq}(\sqrt{\frac{-\hbar_1}{8}}\zeta)]^2\}e^{\rho\mathcal{W}-\frac{1}{2}\rho^2t}, \tag{44}$$

for $\left(\hbar_1-k-3k^2+3\delta\right)>0$.

Case I-4: If $\hbar_1>0$, and $\hbar_2=\frac{\hbar_1^2}{4}$, then

$$\mathcal{Y}_{1,9}=\pm\sqrt{2\hbar_1\left(\hbar_1-k-3k^2+3\delta\right)}\tan_{pq}(\sqrt{\frac{\hbar_1}{2}}\zeta)e^{i\Theta+\rho\mathcal{W}-\frac{1}{2}\rho^2t}, \tag{45}$$

$$\mathcal{Z}_{1,9}=\{k^2-\delta-\hbar_1-\hbar_1\tan_{pq}^2(\sqrt{\frac{\hbar_1}{2}}\zeta)\}e^{\rho\mathcal{W}-\frac{1}{2}\rho^2t}, \tag{46}$$

$$\mathcal{Y}_{1,10}=\pm\sqrt{2\hbar_1\left(\hbar_1-k-3k^2+3\delta\right)}\cot_{pq}(\sqrt{\frac{\hbar_1}{2}}\zeta)e^{i\Theta+\rho\mathcal{W}-\frac{1}{2}\rho^2t}, \tag{47}$$

$$\mathcal{Z}_{1,10}=\{k^2-\delta-\hbar_1-\hbar_1\cot_{pq}^2(\sqrt{\frac{\hbar_1}{2}}\zeta)\}e^{\rho\mathcal{W}-\frac{1}{2}\rho^2t}, \tag{48}$$

$$\mathcal{Y}_{1,11}=\pm\sqrt{2\hbar_1\left(\hbar_1-k-3k^2+3\delta\right)}[\tan_{pq}(\sqrt{2\hbar_1}\zeta)\pm\sqrt{pq}\sec_{pq}(\sqrt{2\hbar_1}\zeta)]e^{i\Theta+\rho\mathcal{W}-\frac{1}{2}\rho^2t}, \tag{49}$$

$$\mathcal{Z}_{1,11}=\{k^2-\delta-\hbar_1-\hbar_1[\tan_{pq}(\sqrt{2\hbar_1}\zeta)\pm\sqrt{pq}\sec_{pq}(\sqrt{2\hbar_1}\zeta)]^2\}e^{\rho\mathcal{W}-\frac{1}{2}\rho^2t}, \tag{50}$$

$$\mathcal{Y}_{1,12}=\pm\sqrt{2\hbar_1\left(\hbar_1-k-3k^2+3\delta\right)}[\cot_{pq}(\sqrt{2\hbar_1}\zeta)\pm\sqrt{pq}\csc_{pq}(\sqrt{2\hbar_1}\zeta)]e^{i\Theta+\rho\mathcal{W}-\frac{1}{2}\rho^2t}, \tag{51}$$

$$\mathcal{Z}_{1,12}=\{k^2-\delta-\hbar_1-\hbar_1[\cot_{pq}(\sqrt{2\hbar_1}\zeta)\pm\sqrt{pq}\csc_{pq}(\sqrt{2\hbar_1}\zeta)]^2\}e^{\rho\mathcal{W}-\frac{1}{2}\rho^2t}, \tag{52}$$

and

$$\mathcal{Y}_{1,13}=\pm\frac{1}{2}\sqrt{\hbar_1\left(\hbar_1-k-3k^2+3\delta\right)}[\tan_{pq}(\sqrt{\frac{\hbar_1}{8}}\zeta)+\cot_{pq}(\sqrt{\frac{\hbar_1}{8}}\zeta)]e^{i\Theta+\rho\mathcal{W}-\frac{1}{2}\rho^2t}, \tag{53}$$

$$\mathcal{Z}_{1,13}=\{k^2-\delta-\hbar_1-\frac{\hbar_1}{4}[\tan_{pq}(\sqrt{\frac{\hbar_1}{8}}\zeta)+\cot_{pq}(\sqrt{\frac{\hbar_1}{8}}\zeta)]^2\}e^{\rho\mathcal{W}-\frac{1}{2}\rho^2t}, \tag{54}$$

for $\left(\hbar_1-k-3k^2+3\delta\right)>0$.

Remark 1. *Putting $p=q=1$, $\rho=0$ and $\alpha=1$ from (29) to (54) yields the identical results as those expressed in [16].*

Set II: Putting (26) into Eq. (24), we get the following solution for the traveling wave Eq. (8):

$$\begin{aligned} u(\eta) &= 2\sqrt{2}\left(10\hbar_1 - \sqrt{\hbar_1 - 3\hbar_2}\right) + 6\sqrt{2}\mathcal{M}^2(\eta), \\ v(\eta) &= -(2\hbar_1 + \frac{1}{3}k + \frac{4}{3}\sqrt{\hbar_1 - 3\hbar_2}) - 6\mathcal{M}^2(\eta). \end{aligned} \tag{55}$$

Consequently, setting Eq. (55) into Eq. (2), we obtain the solutions of the SCS-KdVEs-CDO (1) for $\hbar_1 \geq 3\hbar_2$ as follows:

$$\begin{aligned} \mathcal{Y} &= [2\sqrt{2}\left(10\hbar_1 - \sqrt{\hbar_1 - 3\hbar_2}\right) + 6\sqrt{2}\mathcal{M}^2(\eta)]e^{i\Theta + \rho\mathcal{B} - \frac{1}{2}\rho^2 t}, \\ \mathcal{Z} &= -[2\hbar_1 + \frac{1}{3}k + \frac{4}{3}\sqrt{\hbar_1 - 3\hbar_2} + 6\mathcal{M}^2(\eta)]e^{\rho\mathcal{B} - \frac{1}{2}\rho^2 t}, \end{aligned} \tag{56}$$

where $\eta = \frac{1}{\alpha}x^\alpha + 2kt$ and $\Theta = \frac{k}{\alpha}x^\alpha + \delta t$.

Now, substituting from Eqs (11) to (23) into Eq. (56), we have the next solutions of the SCS-KdVEs-CDO (1):

Case II-1: If $\hbar_1 > 0$, and $\hbar_2 = 0$, then

$$\mathcal{Y}_{2,1} = [18\sqrt{2}\hbar_1 + 6\sqrt{2}\mathrm{sech}^2_{pq}(\sqrt{\hbar_1}\zeta)]e^{i\Theta + \rho\mathcal{W} - \frac{1}{2}\rho^2 t}, \tag{57}$$

$$\mathcal{Z}_{2,1} = -[\frac{10}{3}\hbar_1 + \frac{1}{3}k + 6\mathrm{sech}^2_{pq}(\sqrt{\hbar_1}\zeta)]e^{\rho\mathcal{W} - \frac{1}{2}\rho^2 t}, \tag{58}$$

and

$$\mathcal{Y}_{2,2} = [18\sqrt{2}\hbar_1 + 6\sqrt{2}\mathrm{csch}^2_{pq}(\sqrt{\hbar_1}\zeta)]e^{i\Theta + \rho\mathcal{W} - \frac{1}{2}\rho^2 t}, \tag{59}$$

$$\mathcal{Z}_{2,2} = -[\frac{10}{3}\hbar_1 + \frac{1}{3}k + 6\mathrm{csch}^2_{pq}(\sqrt{\hbar_1}\zeta)]e^{\rho\mathcal{W} - \frac{1}{2}\rho^2 t}. \tag{60}$$

Case II-2: If $\hbar_1 < 0$, and $\hbar_2 = 0$, then

$$\mathcal{Y}_{2,3} = [22\sqrt{2}\hbar_1 + 6\sqrt{2}\sec^2_{pq}(\sqrt{-\hbar_1}\zeta)]e^{i\Theta + \rho\mathcal{W} - \frac{1}{2}\rho^2 t}, \tag{61}$$

$$\mathcal{Z}_{2,3} = -[\frac{2}{3}\hbar_1 + \frac{1}{3}k + 6\sec^2_{pq}(\sqrt{-\hbar_1}\zeta)]e^{\rho\mathcal{W} - \frac{1}{2}\rho^2 t}, \tag{62}$$

and

$$\mathcal{Y}_{2,4} = [22\sqrt{2}\hbar_1 + 6\sqrt{2}\csc^2_{pq}(\sqrt{-\hbar_1}\zeta)]e^{i\Theta + \rho\mathcal{W} - \frac{1}{2}\rho^2 t}, \tag{63}$$

$$\mathcal{Z}_{2,4} = -[\frac{2}{3}\hbar_1 + \frac{1}{3}k + 6\csc^2_{pq}(\sqrt{-\hbar_1}\zeta)]e^{\rho\mathcal{W} - \frac{1}{2}\rho^2 t}. \tag{64}$$

Case II-3: If $\hbar_1 < 0$, and $\hbar_2 = \frac{\hbar_1^2}{4}$, then

$$\mathcal{Y}_{2,5} = [19\sqrt{2}\hbar_1 + 6\sqrt{2}\tanh^2_{pq}(\sqrt{\frac{-\hbar_1}{2}}\zeta)]e^{i\Theta + \rho\mathcal{W} - \frac{1}{2}\rho^2 t}, \tag{65}$$

$$\mathcal{Z}_{2,5} = -[\frac{1}{3}k + \frac{4}{3}\hbar_1 + 6\tanh^2_{pq}(\sqrt{\frac{-\hbar_1}{2}}\zeta)]e^{\rho\mathcal{W} - \frac{1}{2}\rho^2 t}, \tag{66}$$

$$\mathcal{Y}_{2,6}=[19\sqrt{2}\hbar_1+6\sqrt{2}\coth_{pq}^2(\sqrt{\frac{-\hbar_1}{2}}\zeta)]e^{i\Theta+\rho\mathcal{W}-\frac{1}{2}\rho^2t}, \tag{67}$$

$$\mathcal{Z}_{1,6}=[\frac{1}{3}k+\frac{4}{3}\hbar_1+6\coth_{pq}^2(\sqrt{\frac{-\hbar_1}{2}}\zeta)]e^{\rho\mathcal{W}-\frac{1}{2}\rho^2t}, \tag{68}$$

$$\mathcal{Y}_{2,7}=[19\sqrt{2}\hbar_1+6\sqrt{2}(\coth_{pq}(\sqrt{-2\hbar_1}\zeta)\pm\sqrt{pq}\mathrm{csch}_{pq}(\sqrt{-2\hbar_1}\zeta))^2]e^{i\Theta+\rho\mathcal{W}-\frac{1}{2}\rho^2t}, \tag{69}$$

$$\mathcal{Z}_{2,7}=-[\frac{1}{3}k+\frac{4}{3}\hbar_1+6(\coth_{pq}(\sqrt{-2\hbar_1}\zeta)\pm\sqrt{pq}\mathrm{csch}_{pq}(\sqrt{-2\hbar_1}\zeta))^2]e^{\rho\mathcal{W}-\frac{1}{2}\rho^2t}, \tag{70}$$

and

$$\mathcal{Y}_{2,8}=[19\sqrt{2}\hbar_1+6\sqrt{2}(\tanh_{pq}(\sqrt{\frac{-\hbar_1}{8}}\zeta)+\coth_{pq}(\sqrt{\frac{-\hbar_1}{8}}\zeta))^2]e^{i\Theta+\rho\mathcal{W}-\frac{1}{2}\rho^2t}, \tag{71}$$

$$\mathcal{Z}_{2,8}=-[\frac{1}{3}k+\frac{4}{3}\hbar_1+6(\tanh_{pq}(\sqrt{\frac{-\hbar_1}{8}}\zeta)+\coth_{pq}(\sqrt{\frac{-\hbar_1}{8}}\zeta))^2]e^{\rho\mathcal{W}-\frac{1}{2}\rho^2t}. \tag{72}$$

Case II-4: If $\hbar_1>0$, and $\hbar_2=\frac{\hbar_1^2}{4}$, then

$$\mathcal{Y}_{2,9}=[19\sqrt{2}\hbar_1+6\sqrt{2}\tan_{pq}^2(\sqrt{\frac{\hbar_1}{2}}\zeta)]e^{i\Theta+\rho\mathcal{W}-\frac{1}{2}\rho^2t}, \tag{73}$$

$$\mathcal{Z}_{2,9}=-[\frac{8}{3}\hbar_1+\frac{1}{3}k+6\tan_{pq}^2(\sqrt{\frac{\hbar_1}{2}}\zeta)]e^{\rho\mathcal{W}-\frac{1}{2}\rho^2t}, \tag{74}$$

$$\mathcal{Y}_{2,10}=[19\sqrt{2}\hbar_1+6\sqrt{2}\cot_{pq}^2(\sqrt{\frac{\hbar_1}{2}}\zeta)]e^{i\Theta+\rho\mathcal{W}-\frac{1}{2}\rho^2t}, \tag{75}$$

$$\mathcal{Z}_{2,10}=-[\frac{8}{3}\hbar_1+\frac{1}{3}k+6\cot_{pq}^2(\sqrt{\frac{\hbar_1}{2}}\zeta)]e^{\rho\mathcal{W}-\frac{1}{2}\rho^2t}, \tag{76}$$

$$\mathcal{Y}_{2,11}=[19\sqrt{2}\hbar_1+6\sqrt{2}(\tan_{pq}(\sqrt{2\hbar_1}\zeta)\pm\sqrt{pq}\sec_{pq}(\sqrt{2\hbar_1}\zeta))^2]e^{i\Theta+\rho\mathcal{W}-\frac{1}{2}\rho^2t}, \tag{77}$$

$$\mathcal{Z}_{2,11}=-[\frac{8}{3}\hbar_1+\frac{1}{3}k+6(\tan_{pq}(\sqrt{2\hbar_1}\zeta)\pm\sqrt{pq}\sec_{pq}(\sqrt{2\hbar_1}\zeta))^2]e^{\rho\mathcal{W}-\frac{1}{2}\rho^2t}, \tag{78}$$

$$\mathcal{Y}_{2,12}=[19\sqrt{2}\hbar_1+6\sqrt{2}(\cot_{pq}(\sqrt{2\hbar_1}\zeta)\pm\sqrt{pq}\csc_{pq}(\sqrt{2\hbar_1}\zeta))^2]e^{i\Theta+\rho\mathcal{W}-\frac{1}{2}\rho^2t}, \tag{79}$$

$$\mathcal{Z}_{2,12}=-[\frac{8}{3}\hbar_1+\frac{1}{3}k+6(\cot_{pq}(\sqrt{2\hbar_1}\zeta)\pm\sqrt{pq}\csc_{pq}(\sqrt{2\hbar_1}\zeta))^2]e^{\rho\mathcal{W}-\frac{1}{2}\rho^2t}, \tag{80}$$

and

$$\mathcal{Y}_{2,13}=[19\sqrt{2}\hbar_1+6\sqrt{2}(\tan_{pq}(\sqrt{\frac{\hbar_1}{8}}\zeta)+\cot_{pq}(\sqrt{\frac{\hbar_1}{8}}\zeta))^2]e^{i\Theta+\rho\mathcal{W}-\frac{1}{2}\rho^2t}, \tag{81}$$

$$\mathcal{Z}_{2,13}=-[\frac{8}{3}\hbar_1+\frac{1}{3}k+6(\tan_{pq}(\sqrt{\frac{\hbar_1}{8}}\zeta)+\cot_{pq}(\sqrt{\frac{\hbar_1}{8}}\zeta))^2]e^{\rho\mathcal{W}-\frac{1}{2}\rho^2t}. \tag{82}$$

Remark 2. *Putting $p=q=1$, $\rho=0$ and $\alpha=1$ from (57) to (82) yields the identical results as those expressed in [21].*

5. Effect of Noise and Fractional Derivatives

The recent advances in experimental techniques and numerical simulations of nonlinear wave dynamics offer the possibility of confirming the analytical results presented in this study. In particular, the bright and dark soliton solutions obtained herein under the influence of stochasticity can serve as test beds for the validation of numerical approaches to noisy fractional systems. For instance, the application of fractional spectral methods and stochastic finite-difference techniques can model the same conditions and be contrasted with our exact solutions in order to understand the robustness and validity of computational approaches. Additionally, in experimental settings such as nonlinear optics and Bose-Einstein condensates, setups with tunable noise and dispersion parameters can provide feasible arenas for tracking the qualitative dynamics predicted by our work. Hence, our results not only enrich the theory of nonlinear FPDEs but also pave the way for future experimental verification and numerical exploration.

Effect of Noise: The existence of multiplicative noise in the Schrödinger-KdV equation can have significant implications for the dynamics of the system. In the presence of noise, the solutions of the equation may exhibit stochastic behavior, leading to fluctuations in the amplitude and phase of the waves. These fluctuations can affect the stability of the solutions and the overall dynamics of the system, making it challenging to accurately predict the behavior of the waves over time.

Let us now display the noise impacts on the exact solution of the SCS-KdVEs-CDO (1). Many figures are included to illustrate the behavior of some of the solutions that were produced, such as Eqs (29), (30), (37), and (38) as follows:

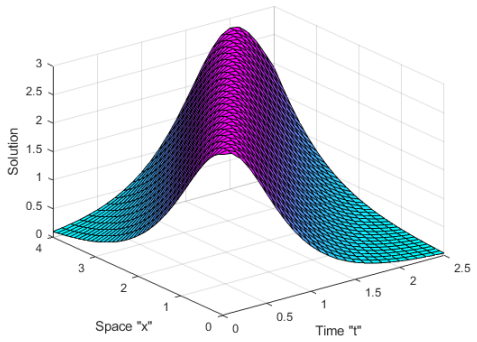

(a) $\rho = 0$

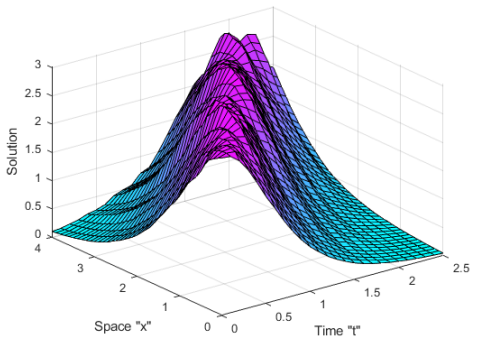

(b) $\rho = 0.1$

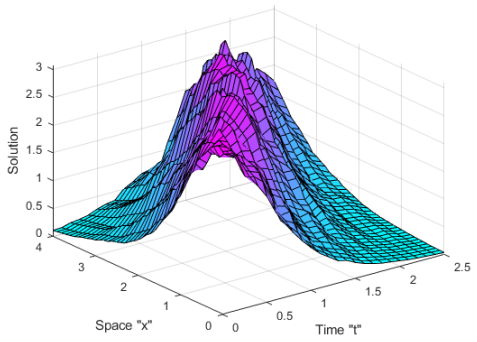

(c) $\rho = 0.3$

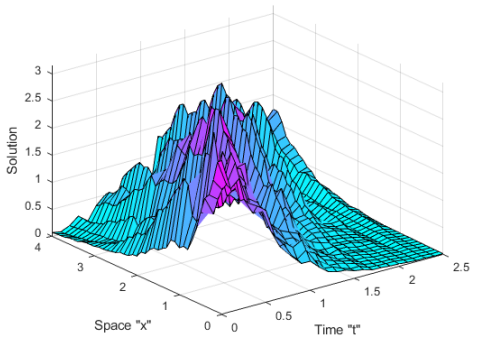

(d) $\rho = 1$

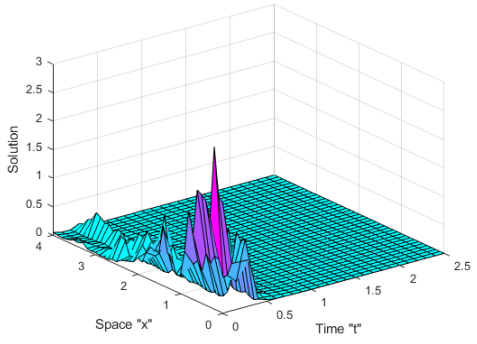

(e) $\rho = 2$

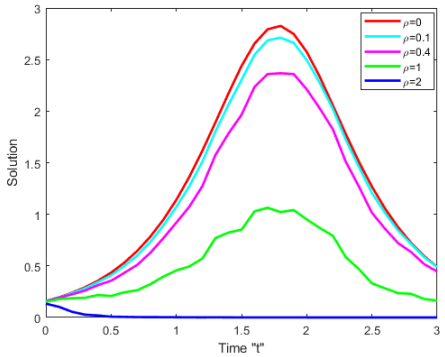

(f) $\rho = 0,\ 0.1,\ 0.3,\ 1,\ 2$

Figure 1. (a-e) 3D profiles of the bright soliton solution $\mathcal{Y}(x,t)$ of Eq. (29) under different noise intensities ρ. As ρ increases from 0 to 2, the soliton peak deforms significantly: small noise ($\rho = 0.1, 0.3$) induces slight oscillations, while stronger noise ($\rho = 1, 2$) destabilizes and suppresses the soliton, reflecting the dissipative role of stochasticity. (f) 2D cross-sectional profiles showing how increasing ρ reduces amplitude and broadens the wave, indicating that noise progressively stabilizes the solution toward zero. Simulations are performed with $k = -1,\ q = 0.8,\ p = 0.9,\ \delta = 1,\ x \in [0, 4]$,

$t \in [0, 2.5]$, and derivative order $\alpha = 1$.

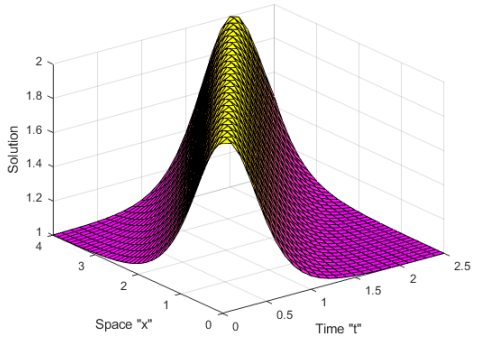

(a) $\rho = 0$

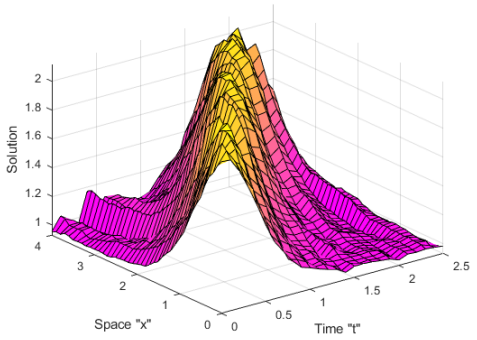

(b) $\rho = 0.1$

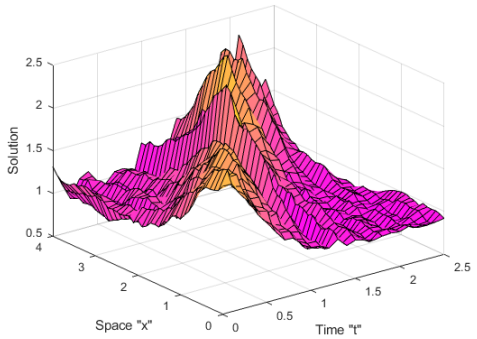

(c) $\rho = 0.3$

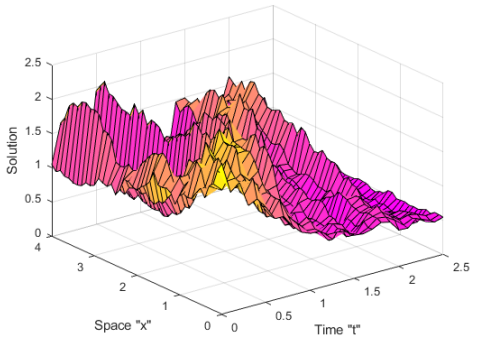

(d) $\rho = 1$

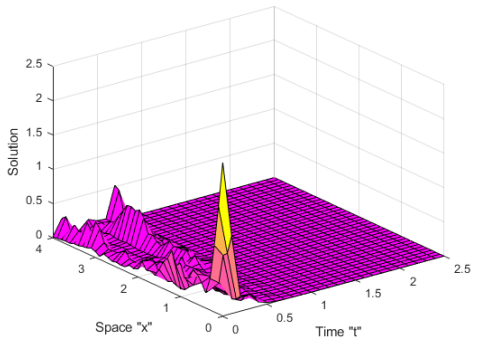

(e) $\rho = 2$

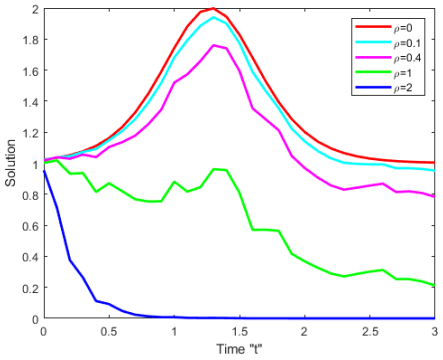

(f) $\rho = 0,\ 0.1,\ 0.3,\ 1,\ 2$

Figure 2. (a-e) 3D views of the bright soliton solution $\mathcal{Z}(x,t)$ of Eq. (30) under varying noise intensities $\rho = 0, 0.1, 0.3, 1, 2$. Thes plots are drawn when $k = -1,\ q = 0.8,\ p = 0.9,\ \delta = 1,\ x \in [0, 4],\ t \in [0, 2.5]$.

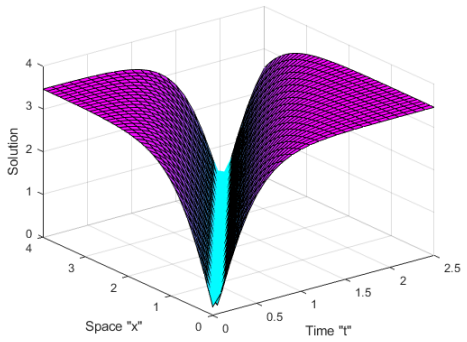

(a) $\rho = 0$

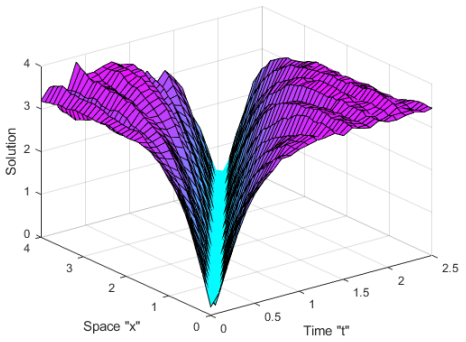

(b) $\rho = 0.1$

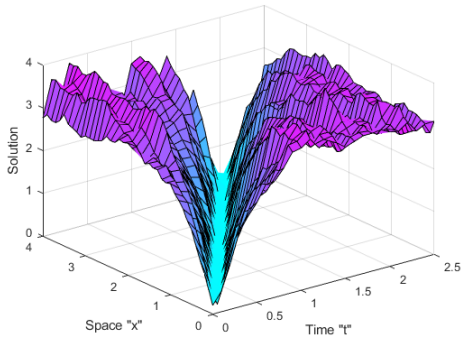

(c) $\rho = 0.3$

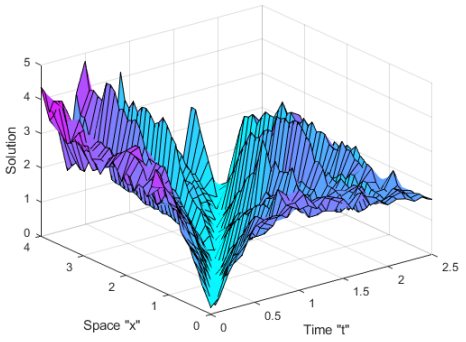

(d) $\rho = 1$

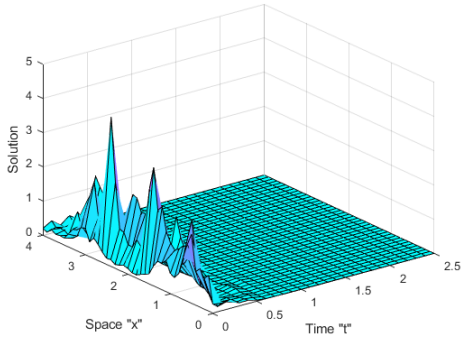

(e) $\rho = 2$

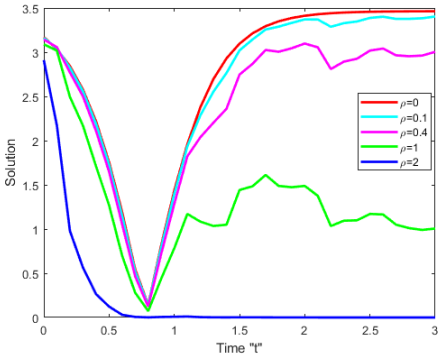

(f) $\rho = 0,\ 0.1,\ 0.3,\ 1,\ 2$

Figure 3. (a-e) 3D profiles of the dark soliton solution $\mathcal{Y}(x,t)$ of Eq. (37) for different noise strengths $\rho = 0, 0.1, 0.3, 1, 2$. Thes plots are drawn when $k = -1,\ q = 0.8,\ p = 0.9,\ \delta = 1,\ x \in [0,4],\ t \in [0,2.5]$.

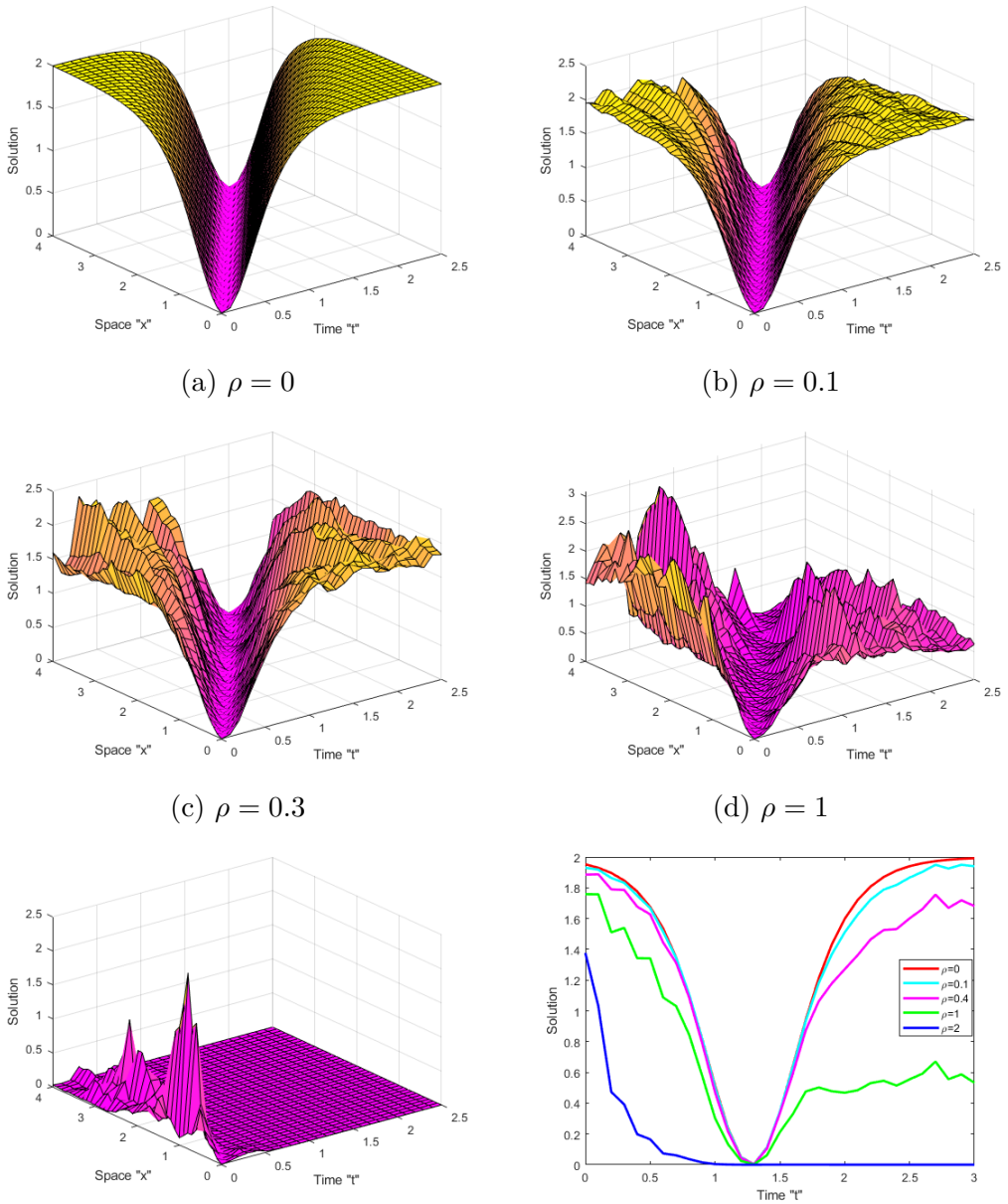

(a) $\rho = 0$ (b) $\rho = 0.1$

(c) $\rho = 0.3$ (d) $\rho = 1$

(e) $\rho = 2$ (f) $\rho = 0,\ 0.1,\ 0.3,\ 1,\ 2$

Figure 4.(a-e) The 3D plots present the dark soliton solution $\mathcal{Z}(x,t)$ of Eq. (38) under varying noise intensities $\rho = 0, 0.1, 0.3, 1, 2$. Thes plots are drawn when $k = -1,\ q = 0.8,\ p = 0.9,\ \delta = 1,\ x \in [0,4],\ t \in [0,2.5]$.

Now, Figures 1-4 show some different kinds of solutions, such as bright soliton, dark soliton solutions, when the multiplicative noise is disregarded (i.e. when $\rho = 0$). When noise is introduced and its amplitude is increased by $\rho = 0.1,\ 0.3,\ 1,\ 2$, the surface flattens out after brief transit patterns. This indicates that the solutions of the SCS-KdVEs-CDO

are impacted by multiplicative noise and are kept stable around zero.

Effect of Fractional derivatives: The presence of conformable derivative operator in the Schrödinger-KdV equation allows for a more accurate and comprehensive description of wave propagation in one-dimensional media. By incorporating fractional derivatives, researchers can better understand the complex dynamics and emergent behavior that arise in nonlinear systems. This highlights the importance of considering fractional calculus in the study of physical phenomena, and suggests that it may play a key role in the development of future models and theories in physics and applied mathematics.

The leftward displacement of wave profiles with decreasing fractional order α signifies a fundamental alteration of propagation dynamics, in direct result of the memory and hereditary effects introduced by the fractional derivative. Physically, the displacement reflects the reduction of the effective wave speed and the enhancement of attenuation, as the non-local operator $\frac{\partial^\alpha}{\partial t^\alpha}$ imposes more dissipation and frequency-dependent dispersion, characteristics shared with the propagation of waves in complex viscoelastic media. Mathematically, the enhanced sensitivity of the system to its previous history hinders the advancement of the wave, which appears as an apparent forward shift of the waveform that demonstrates the model's ability to capture anomalous transport behavior.

Now, let us show the effect of the conformable derivative operator on the exact solution of the SCS-KdVEs-CDO (1). To address the behavior of some of the obtained solutions, many figures are provided, such as Eqs (29), (30), (37), and (38) as follows:

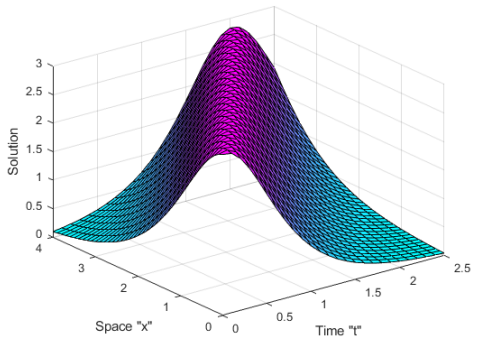

(a) $\alpha = 1,\ \rho = 0,$

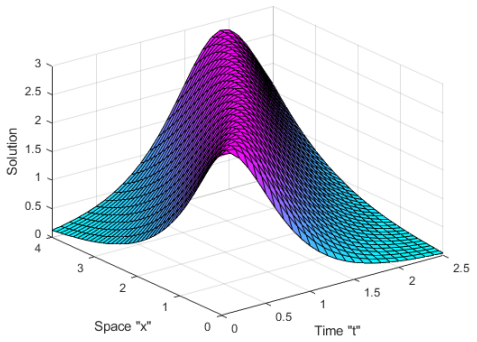

(b) $\alpha = 0.8,\ \rho = 0,$

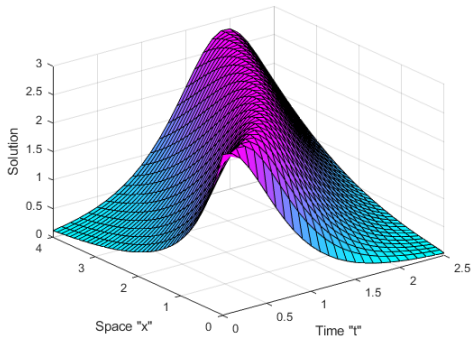

(c) $\alpha = 0.6,\ \rho = 0,$

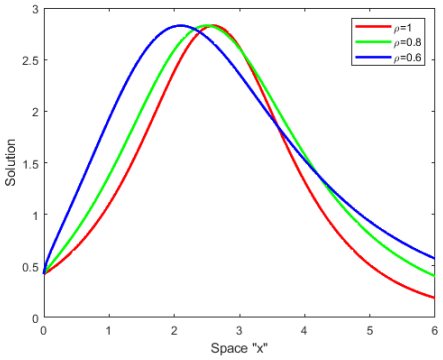

(d) $\alpha = 1,\ 0.8,\ 0.6$ and $\rho = 0,$

Figure 5. (a-c) exhibit 3D-profile of solution $\mathcal{Y}(x,t)$ in Eq (29) with $k = -1,\ q = 0.8,\ p = 0.9,\ \delta = 1,\ x \in [0,4],\ t \in [0,2.5]$ and $\rho = 0$, (d) shows 2D-profile of Eq. (29) with different α demonstrating how reducing the fractional derivative order α attenuates the wave amplitude and smooths the wave profile.

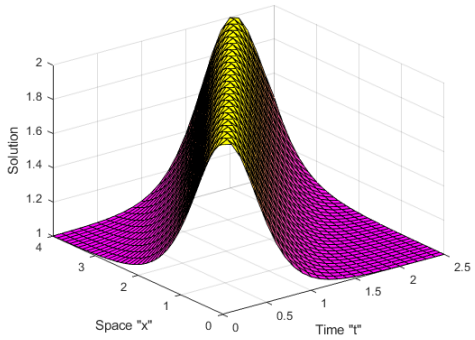

(a) $\alpha = 1,\ \rho = 0,$

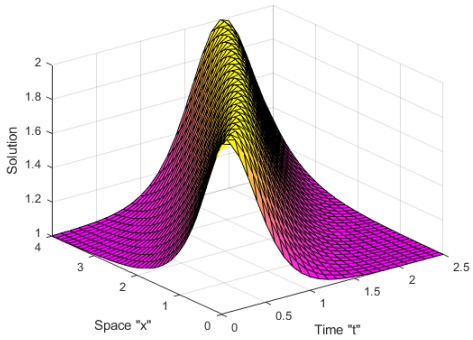

(b) $\alpha = 0.8,\ \rho = 0,$

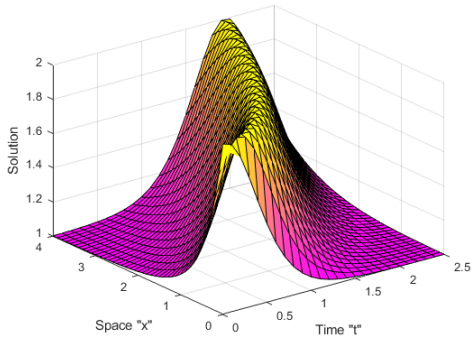

(c) $\alpha = 0.6,\ \rho = 0,$

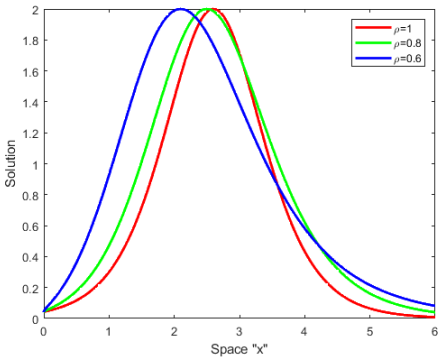

(d) $\alpha = 1,\ 0.8,\ 0.6$ and $\rho = 0,$

Figure 6. (a-c) exhibit 3D-profile of solution $\mathcal{Z}(x,t)$ in Eq. (30) with $k = -1,\ q = 0.8,\ p = 0.9,\ \delta = 1,\ x \in [0,4],\ t \in [0,2.5]$ and $\rho = 0$ (d) 2D profile which demonstrating that a reduction in the fractional derivative order α introduces significant

diffusivity, smoothing sharp wave features and reducing peak intensity, which reflects enhanced dissipative behavior typical of fractional-order systems in physical contexts such as anomalous diffusion or viscoelastic damping for Eq. (30.

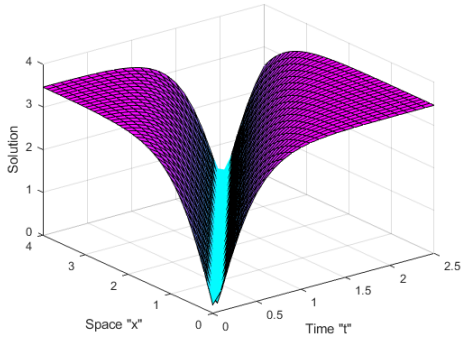

(a) $\alpha = 1,\ \rho = 0,$

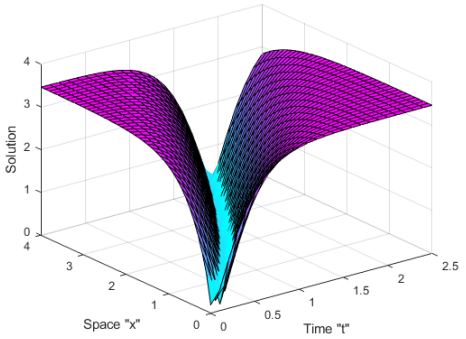

(b) $\alpha = 0.8,\quad \rho = 0,$

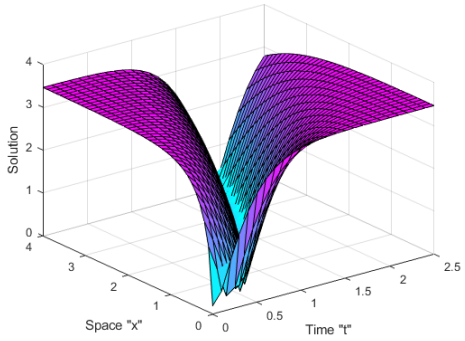

(c) $\alpha = 0.6,\ \rho = 0,$

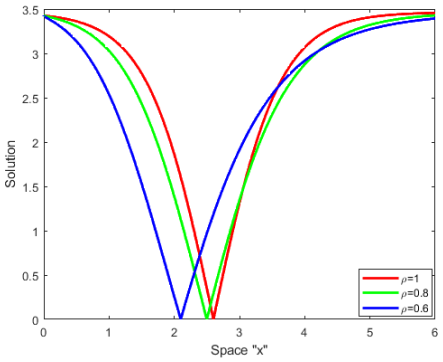

(d) $\alpha = 1,\ 0.8,\ 0.6$ and $\rho = 0$

Figure 7. (a-c) exhibit 3D-profile of solution $\mathcal{Y}(x,t)$ in Eq. (37) with $k = -1,\ q = 0.8,\ p = 0.9,\ \delta = 1,\ x \in [0,4]$, $t \in [0,2.5]$ and $\rho = 0$ (d) 2D profile showing that decreasing α dampens wave oscillations and flattens the amplitude of Eq. (37).

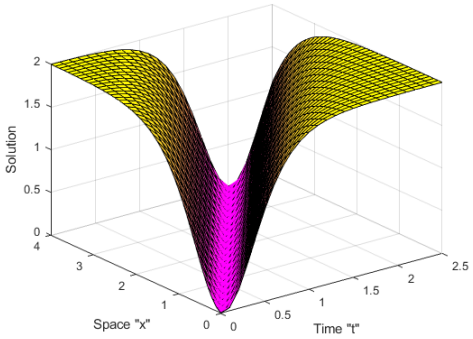

(a)$\alpha = 1,\ \rho = 0,$

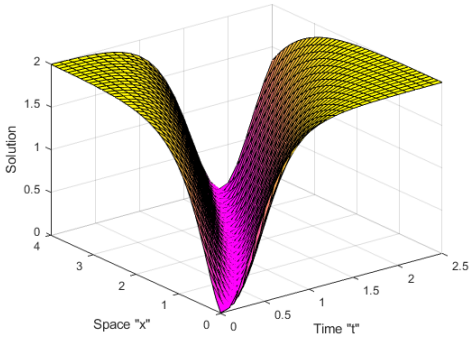

(b) $\alpha = 0.8,\quad \rho = 0,$

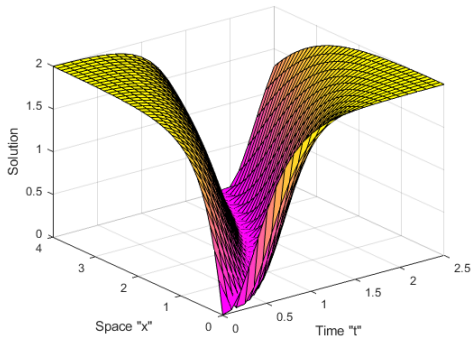

(c) $\alpha = 0.6, \quad \rho = 0,$

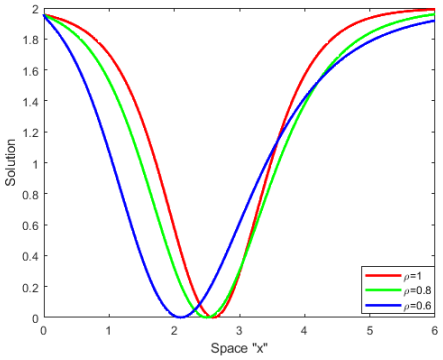

(d) $\alpha = 1,\ 0.8,\ 0.6$ and $\rho = 0,$

Figure 8. (a-c) exhibit the 3D profile of solution $\mathcal{Z}(x,t)$ in Eq. (38) with $k = -1,\ q = 0.8,\ p = 0.9,\ \delta = 1,\ x \in [0,4]$, $t \in [0, 2.5]$ and $\rho = 0$ (d) 2D profile showing that decreasing α dampens wave oscillations and flattens the amplitude of Eq. (38).

From the previous Figures $5-8$, we conclude that the surface shifts to the left as the derivative order α of conformable derivative operator decreases.

Physical meaning: The SCS-KdVEs-CDO (1) represent a compelling intersection between quantum mechanics, nonlinear dynamics, and fractional calculus. It describes a generalization of the classical Schrödinger equation combined with the KdV equation, incorporating random perturbations and fractional derivatives. Therefore, the obtained solutions for these equations are very important. We obtained various soliton solutions, including a periodic soliton, a bright soliton, a dark-bright soliton and a singular soliton solution, by using the Sardar subequation method. The soliton solutions of the Schrödinger-KdV equation have implications for quantum field theory and soliton theory itself. In quantum mechanics, certain soliton states can represent bound states of particles, providing a novel perspective on particle interactions in quantum fields. The integrability properties of the Schrödinger-KdV equation allow physicists to derive exact solutions, facilitating the exploration of new physical phenomena such as rogue waves and soliton gas formations. These solutions can aid in the mathematical formulation of highly non-linear dynamics and enrich our theoretical understanding of nature, where complex interactions often lead to emergent phenomena.

6. Conclusions

In this paper, the stochastic coupled Schrödinger-KdV equations with conformable derivative operator (1) were considered. By using the Sardar subequation method, we were able to obtain a periodic soliton, a bright soliton, a dark-bright soliton, and a singular soliton solution. When $\rho = 0$ and $\alpha = 1$, we get some previously known solutions of the SCS-KdVEs-CDO (1) as stated in previous remarks. These obtained solutions may be beneficial, practical, and can explain a wide variety of crucial physical phenomena because the SCS-KdVEs-CDO equations have significant uses in dusty plasma, including

Langmuir, electromagnetic waves, and dust-acoustic waves. Compared to former deterministic approaches such as the Petrov-Galerkin approach for coupled Schrödinger-KdV equations [20] and Sardar sub-equation approach for the Boussinesq equation [26], the present paper provides a broader solution space. Exactly, new solution patterns, perverse as well as systematic extensions of the conformable deterministic counterpart ($\rho = 0$) are all encompassed in our results, which thereby demonstrates the novelty of the proposed method. Additionally, by drawing several graphs in both two and three dimensions using the MATLAB program (version R2022b), the effects of the conformable derivative operator and noise term on the analytical solution of the SCS-KdVEs-CDO (1) were studied. We showed that the multiplicative Wiener process stabilized the solutions around zero, while the conformable derivative operator shifts the surface to the left when the derivative order α decreases. We can investigate the exact solutions of coupled Schrödinger-KdV equations with additive noise in further research.

Acknowledgements

This research has been funded by Scientific Research Deanship at the University of Ha'il-Saudi Arabia through project number RG-25050.

References

[1] Haci Mehmet Baskonus, Hasan Bulut, and Tukur Abdulkadir Sulaiman. New complex hyperbolic structures to the lonngren-wave equation by using sine-gordon expansion method. *Applied Mathematics & Nonlinear Sciences*, 4(1), 2019.

[2] Wael W Mohammed, Clemente Cesarano, Naveed I. Alqsair, and Rabeb Sidaoui. The impact of brownian motion on the optical solutions of the stochastic ultra-short pulses mathematical model. *Alexandria Engineering Journal*, 101:186–192, 2024.

[3] Mohammad Alshammari, Amjad E Hamza, Clemente Cesarano, Elkhateeb S Aly, and Wael W Mohammed. The analytical solutions to the fractional kraenkel–manna–merle system in ferromagnetic materials. *Fractal and Fractional*, 7(7):523, 2023.

[4] Wael W. Mohammed, Monirah W Alshammary, Ahmed E Matouk, and Naveed Iqbal. Abundant solitary solutions for the fractional unidirectional wave model using in oceanography, coastal engineering, and meteorology. *European Journal of Pure and Applied Mathematics*, 18:6422–6422, 2025.

[5] Mingliang Wang, Xiangzheng Li, and Jinliang Zhang. The $(g'/g)-$expansion method and travelling wave solutions of nonlinear evolution equations in mathematical physics. *Physics Letters A*, 372(4):417–423, 2008.

[6] Huiqun Zhang. New application of the $(g'/g)-$expansion method. *Communications in Nonlinear Science and Numerical Simulation*, 14(8):3220–3225, 2009.

[7] Abdul-Majid Wazwaz. The sine–cosine method for obtaining solutions with compact and noncompact structures. *Applied Mathematics and Computation*, 159(2):559–576, 2004.

[8] Amjad E Hamza, Mohammad Alshammari, D Atta, and Wael W Mohammed. Fractional-stochastic shallow water equations and its analytical solutions. *Results in Physics*, 53:106953, 2023.

[9] Ji-Huan He and Xu-Hong Wu. Exp-function method for nonlinear wave equations. *Chaos, Solitons & Fractals*, 30(3):700–708, 2006.

[10] Kamruzzaman Khan and M Ali Akbar. The exp (- ϕ (ξ))–expansion method for finding travelling wave solutions of vakhnenko–parkes equation. *International Journal of Dynamical Systems and Differential Equations*, 5(1):72–83, 2014.

[11] Farah M Al-Askar, Wael W Mohammed, and Mohammad Alshammari. Impact of brownian motion on the analytical solutions of the space-fractional stochastic approximate long water wave equation. *Symmetry*, 14(4):740, 2022.

[12] Zhenya Yan. Abundant families of jacobi elliptic function solutions of the (2+ 1)-dimensional integrable davey–stewartson-type equation via a new method. *Chaos, Solitons & Fractals*, 18(2):299–309, 2003.

[13] Naveed Iqbal, Safyan Mukhtar, Abdulkafi M. Saeed, Rasool Shah, and Shah Hussain. New solitary and soliton wave solutions of the fractional higgs system using a riccati-bernoulli and bäcklund framework. *Nonlinear Dynamics*, 113:26505–26519, 2025.

[14] M. Mossa Al-Sawalha, Saima Noor, Mohammad Alqudah, Musaad S. Aldhabani, and Roman Ullah. Dynamics of the traveling wave solutions of fractional date–jimbo–kashiwara–miwa equation via riccati–bernoulli sub-ode method through bäcklund transformation. *Fractal and Fraction*, 8:497, 2024.

[15] Roshdi Khalil, Mohammed Al Horani, Abdelrahman Yousef, and Mohammad Sababheh. A new definition of fractional derivative. *Journal of computational and applied mathematics*, 264:65–70, 2014.

[16] Hamood Ur Rehman, Ifrah Iqbal, Suhad Subhi Aiadi, Nabil Mlaiki, and Muhammad Shoaib Saleem. Soliton solutions of klein–fock–gordon equation using sardar subequation method. *Mathematics*, 10(18):3377, 2022.

[17] Dongmei Bai and Luming Zhang. The finite element method for the coupled schrödinger–kdv equations. *Physics Letters A*, 373(26):2237–2244, 2009.

[18] Jonu Lee and Rathinasamy Sakthivel. Exact travelling wave solutions for some important nonlinear physical models. *Pramana*, 80(5):757–769, 2013.

[19] Dogan Kaya and Salah M El-Sayed. On the solution of the coupled schrödinger–kdv equation by the decomposition method. *Physics Letters A*, 313(1-2):82–88, 2003.

[20] MS Ismail, Farida M Mosally, and Khadeejah M Alamoudi. Petrov-galerkin method for the coupled schrödinger-kdv equation. In *Abstract and Applied Analysis*, volume 2014, page 705204, 2014.

[21] Ali Filiz, Mehmet Ekici, and Abdullah Sonmezoglu. F-expansion method and new exact solutions of the schrödinger-kdv equation. *The Scientific World Journal*, 2014:34063, 2014.

[22] Cheng-Lin Bai and Hong Zhao. Complex hyperbolic-function method and its applications to nonlinear equations. *Physics Letters A*, 355(1):32–38, 2006.

[23] Hadi Rezazadeh, Amin Gholami Davodi, and Dariush Gholami. Combined formal periodic wave-like and soliton-like solutions of the conformable schrödinger-kdv equation

using the $g'/g-$expansion technique. *Results in Physics*, 47:106352, 2023.

[24] Md Mashiur Rahhman, Ayrin Aktar, and Kamalesh Chandra Roy. Analytical solutions of nonlinear coupled schrodinger–kdv equation via advance exponential expansion. *American Journal of Mathematical and Computer Modelling*, 3(3):46–51, 2018.

[25] Sofian T Obeidat, Wael W Mohammed, and Mona Anis. Multiple elliptic, hyperbolic and trigonometric stochastic solutions-for the stochastic coupled schrödinger-kdv equations in dusty plasma. *Contemporary Mathematics*, 6:7099–7132, 2025.

[26] Taseer Muhammad, Ahmed A Hamoud, Homan Emadifar, Faraidun K Hamasalh, Hooshmand Azizi, and Masoumeh Khademi. Traveling wave solutions to the boussinesq equation via sardar sub-equation technique. *AIMS Math*, 7(6):11134–11149, 2022.